Quantitative evaluation of alternatively spliced mRNA isoforms by label-free real-time plasmonic sensing

César S. Huertas [a], L. G. Carrascosa[a], S. Bonnal [b,c], J. Valcárcel [b, c, d] and L. M. Lechuga[a]*

[a] Nanobiosensors and Bioanalytical Applications Group, Institut Català de Nanociència i Nanotecnologia (ICN2) CSIC & CIBER-BBN, 08193 Bellaterra, Barcelona, Spain

[b] Centre de Regulació Genòmica, 08003 Barcelona, Spain

[c] Universitat Pompeu Fabra, 08003 Barcelona, Spain

[d] Institució Catalana de Recerca i Estudis Avançats

*corresponding author: laura.lechuga@cin2.es Tel: + 34 93 737 4620

Abstract

Alternative splicing of mRNA precursors enables cells to generate different protein outputs from the same gene depending on their developmental or homeostatic status. Its deregulation is strongly linked to disease onset and progression. Current methodologies for monitoring alternative splicing demand elaborate procedures and often present difficulties in discerning between closely related isoforms, e.g. due to cross-hybridization during their detection. Herein, we report a general methodology using a Surface Plasmon Resonance (SPR) biosensor for label-free monitoring of alternative splicing events in real-time, without any cDNA synthesis or PCR amplification requirements. We applied this methodology to RNA isolated from HeLa cells for the quantification of alternatively spliced isoforms of the *Fas* gene, involved in cancer progression through regulation of programmed cell death. We demonstrate that our methodology is isoform-specific, with virtually no cross-hybridization, achieving limits of detection (LODs) in the picoMolar (pM) range. Similar results were obtained for the detection of the *BCL-X* gene mRNA isoforms. The results were independently validated by RT-qPCR, with excellent concordance in the determination of isoform ratios. The simplicity and robustness of this biosensor technology can greatly facilitate the exploration of alternative splicing biomarkers in disease diagnosis and therapy.

Keywords:

Alternative splicing, mRNA isosoforms, SPR, biosensor, biomarker, diagnosis

1. Introduction

Alternative splicing is a complex process that allows the generation of protein variants from a limited repertoire of protein-coding genes in eukaryotic organisms (Braunschweig et al. 2013; Nilsen and Graveley 2010). In this process, primary transcripts contain regions (exons) that eventually become part of the mature mRNAs, while other intervening sequences (introns) are removed by the process of pre-mRNA splicing. However, depending on the way and the number of exons that are combined in the final transcript, different alternatively spliced mRNAs outputs, and therefore proteins, can be generated, a phenomenon observed in more than 90% of human genes (Pan et al. 2008; Wang and et al. 2008). By selecting different exon combinations, the mechanism of alternative splicing equips the cells with ways to regulate gene expression in order to meet their requirements. Most human genes are alternatively spliced to generate from 5-7 isoforms, producing in some cases up to tens of thousands of variants (Lee and Rio 2015; Nilsen and Graveley 2010). Likewise, alterations in alternative splicing decisions can trigger the onset or influence the progression of many diseases, including cancer (Ghigna et al. 2008; Padgett 2012; Tazi et al. 2009). Cancer cells can remodel their proteome producing those proteins that best fuel growth and spreading of tumors by inducing alternative splicing changes, e.g. in genes that are involved in metabolism, apoptosis, cell cycle control, invasion, metastasis, or angiogenesis (David and Manley 2010). A clear example is the *Fas* gene (Izquierdo et al. 2005). Alternative splicing of *Fas* exon 6 generates two isoforms corresponding to the inclusion (*567* isoform) or skipping (*57* isoform) of this exon (Fig. 1). The pro-apoptotic *567* isoform encodes for a full-length transmembrane protein receptor known as APO-1 (or CD95) that binds to Fas ligand (FasL), therefore activating the characteristic signaling cascade of the extrinsic apoptotic pathway (Krammer 2000).

Exon 6 skipping generates an anti-apoptotic isoform that lacks the trans-membrane domain, producing a soluble protein known as sFas that acts as a decoy in the extra-cellular environment by binding to FasL. This version of *Fas,* which is overexpressed in cancer cells (Cascino et al. 1995; Cheng et al. 1994), contributes to cancer aggressiveness (Owen-Schaub et al. 2000; Owen-Schaub et al. 1998) and its detection has been proposed as a potential biomarker for the early diagnosis of cancer (Boroumand-Noughabi et al. 2010). Therefore, deregulated alternative splicing patterns could be considered as a hallmark of cancer and the identification of alternatively spliced variants as biomarkers could cast light on cancer development (Oltean and Bates 2014). Moreover, modulation of splicing isoforms can be considered as a potential therapeutic approach. Consequently, monitoring of alternative splicing can offer cues for cancer diagnosis and medical care by developing approaches aimed at detecting and eventually reverting the deregulated patterns of alternative splicing (Spitali and Aartsma-Rus 2012).

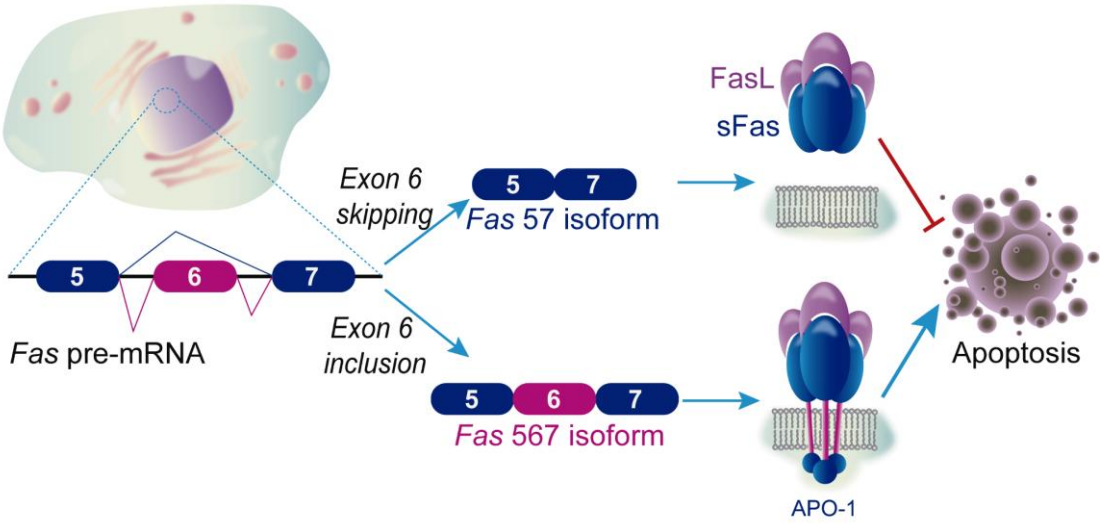

Fig. 1. Schematic representation of the different RNA and protein isoforms generated by alternative splicing of *Fas* gene/*CD95*.

Current methodologies, such as exon microarrays or RNA-Seq, can be used to analyse differences at the exon and/or at transcript variant level, enabling the identification of splicing differences between various types of cancer samples. This isoform-level profiling is yielding more precise cancer signatures than gene-level expression profiles (Zhang et al. 2013). However, microarray-based or RNA-Seq methods are time consuming, expensive and complex for clinical purposes. Methods based on quantitative reverse-transcriptase PCR (RT-qPCR) using exon-specific or splice-junction specific primers (Wu et al. 1996) remain the most suitable approaches. Nevertheless, despite their widespread use, RT-qPCR-based methods are far from fulfilling the needs of routine clinical applications because of the requirement for amplification steps and the use of expensive reagents. Moreover, they often exhibit complications in discerning between closely related isoforms (i.e. isoforms sharing exons or resulting from insertions of a few nucleotides) due to cross-hybridization. Alternative splicing isoforms are intrinsically prone to cross-hybridization (i.e. a not intended binding between a probe and an off-target transcript) which constitutes one of the main sources of systematic error in the study of alternative splicing. The correction of probe-level noise due to cross-hybridization is an indispensable requisite (Xing et al. 2008). Therefore, the avoidance of cross-hybridization significantly increases the reliability of experimental data.

Concerning the analysis of alternative splicing in routine clinical practice, it is necessary to develop a robust methodology to accurately evaluate the expression of the isoforms with minimal operator training and in an easy-to-perform procedure. Currently, single mRNA spliced variants from *BRCA1* gene have been identified and quantified in living cells (Lee et al. 2014). However, one major drawback of this approach is the

requirement of complex and highly specialized optical set-ups and processes that hamper its routine use for diagnosis.

Here, we report a portable Surface Plasmon Resonance (SPR) biosensor for parallel monitoring of alternative splicing events in real-time. SPR biosensor offer significant advantages over conventional techniques enabling analysis with high sensitivity and excellent reproducibility in few minutes. Moreover, it can detect analytes in real time avoiding the use of labels or amplification steps. It represents an user-friendly and robust analytical tool for the analysis of oligonucleotides in minimally-processed samples as previously demonstrated by detection of DNA targets (Li et al. 2007; Vaisocherová et al.) with a specificity up to single mismatches (Carrascosa et al. 2009), and various RNA types, such as microRNAs (Lee et al. 2008; Nasheri et al. 2011; Sipova et al. 2010; Zhou et al. 2011), triplex-forming RNAs (Carrascosa et al. 2012), ribosomal-RNA (Joung et al. 2008; Nelson et al. 2002) as well as other RNA sequences (Boucard et al. 2006; Mandir et al. 2009; Nair et al. 2000). However, to the best of our knowledge, it has never been applied to the direct quantitative analysis of RNA spliced variants. Our methodology permits a rapid (< 20 min) and label-free detection of splicing variants directly from purified total RNA of cells without either cDNA conversion or PCR amplification. In addition, the absence of amplification steps and its reproducibility lead to detections with minimized experimental errors, increasing the reliability of the technique. With a previous and easy-to-implement fragmentation step, we employed this technology to analyze HeLa cell mRNA variants of the *Fas* gene.

2. Materials and methods

2.1. Reagents and HeLa cell RNA samples.

The list of reagents, buffers and solvent used in this work and procedure of preparation of HeLa cell RNA samples is provided in the **Suplementary material**.

2.2. *SPR biosensor.*

We employed a portable home-made SPR sensor as previously described (Carrascosa et al. 2012). The SPR biosensor platform is based on Kretschmann configuration, monitoring the binding events in real time. A p-polarized light of 670 nm from a laser source is divided in two identical beams focused on the crystal-backside of the sensor chip (glass surface coated with 2 nm of chromium and 45 nm of gold, 10x10x0.3 mm, SSens, Enschede –The Netherlands-). Measurements are performed at a fixed angle of incidence. Variations of the refractive index (RI) are detected due to the biointeraction events occurring at the sensor surface as changes in the reflected light intensity by a multielement photodiode. The flow system consists of two flow cells (300 nL each) for independent analysis. The device incorporates all optics, electronics and fluidics components necessary to operate autonomously. Sensograms reproduce the binding event by monitoring the increase (or decrease in case of unbinding events) of the intensity of the reflected light (ΔReflectivity (%), ΔR (%)) vs. time (seconds, s). This change of the intensity of the reflected light is directly related to changes in the RI of the dielectric medium caused by mass changes on the metallic surface.

To prevent from RNAse activity during measurements, the microfluidic sensor was cleaned by flowing sequentially SDS 0.5%, HCl 0.1 M, EtOH 100% and sterile H_2O. All solid materials were autoclaved at 121ºC/20 min for plastic and 134ºC/10 min for glass.

2.3. *DNA-probes immobilization.*

Prior to DNA-probe immobilization, gold sensor chips were cleaned by consecutive sonication cycles (1 min) with solvents of decreasing polarity (i.e. acetone, ethanol and dH_2O) previously heated up to their boiling point. Then, substrates are dried under nitrogen flux and placed in an UV/O3 generator (BioForce Nanosciences, USA) for 20 min. After that, gold sensor chips are subsequently rinsed with ethanol and water and dried under nitrogen flux. The gold sensor chip is then placed into the SPR device.

Formation of mixed self-assembled monolayers (SAMs) of DNA-probe/MCH (1 μM) was carried out *in-situ* on the gold sensor chip by flowing 250 μL of the mix in PB buffer solution at a 12 μL/min rate. Different DNA-probe/MCH molar ratios (no MCH, 10:1 and 20:1) were employed depending on the experiment carried out.

2.4. *Isoforms hybridization and biosensor regeneration.*

Splicing variants detection was performed by injection of the target splicing variant samples into the SPR biosensor at a 16 μL/min rate and subsequent hybridization with their complementary DNA-probes immobilized on the sensor surface. These samples were dissolved in either 5xSSC (0.75 M in NaCl, 0.075 M in sodium citrate) or 3xSSC (0.45 M in NaCl, 0.045 M in sodium citrate). Different concentrations of Formamide ≥99.5% (Sigma Aldrich, Steinhem – Germany-) were used for improving specificity. Isoform-probe interactions were disrupted by using a 50% formamide in aqueous solution (Fuchs et al. 2010). Calibration curves were obtained for each DNA-probe by obtaining triplicates measurement of different target dilutions from standards of known concentration. The mean and the standard deviation (SD) of each concentration were plotted versus the target concentration and fitted to a curve.

2.5. *Data analysis.*

The data were analyzed using Origin 8.0 software (OriginLab, Northampton, MA). The experimental detection limit (LOD) was defined as the target concentration giving a ΔR (%) in the hybridization signal at least three times higher than that of the standard deviation of the DNA/RNA control signal. Limit of quantification (LOQ) was defined as the target concentration giving ΔR (%) in the hybridization signal at least ten times higher than that of the standard deviation of the DNA control or the RNA control signal. The coefficients of variation were obtained as the ratio of the standard deviation to the mean, expressed in percentages (*%CV*). Individual assay variation was calculated after analysis of three replicates of the target

at different concentrations. Inter-assays variations were calculated gathering together all three replicates from the individual assays obtained from two different operators. Percentages of cross-hybridization were calculated by dividing the average signal intensity of the off-targets into the average signal intensity of the complementary isoform. Agreement between RT-qPCR and SPR was assessed by applying the Bland-Altman model for replicate measurements.

3. Results and discussion

3.1. Fas gene alternative splicing biosensing: Optimization and assessment

Our main objective was to develop a general, fast and user-friendly methodology for the label-free and PCR-free detection and quantification of alternatively spliced variants in real-time. We used a portable custom-designed biosensor device based on Surface Plasmon Resonance (SPR) technology (Carrascosa et al. 2012). We chose the well-characterized alternative splicing of *Fas* gene as a model system. Since splice-junctions (i.e. complementary to exon sequences flanking the splice junction) represent a unique sequence feature of each transcript, we designed two DNA-probes specifically matching the splice-junctions of each of the *Fas* gene isoforms. To enable the parallel analysis of the isoforms from purified HeLa cell RNA, we biofunctionalized each SPR sensor cell with one of the DNA-probes (Fig. 2A). We carefully optimized biofunctionalization and detection conditions using ~140-200 nucleotide-length DNA versions of both isoforms, i.e. *Fas567* and *Fas57*, containing the exons of interest (exons 5, 6 and 7 in one case, exons 5 and 7 in the other) (**Table S1**).

In order to ensure and maximize the target capture, we compared mixed solutions of the thiol-modified DNA-probes and alkanethiol 6-mercapto-1-hexanol (MCH), a commonly used backfiller that acts as a lateral spacer, improving the target accessibility by minimizing steric hindrance forces (Carrascosa et al. 2009). We chose three different DNA-probe/MCH ratios (zero MCH, 20:1 and 10:1), generating mixed self-assembled

monolayers (SAMs) (Sakao et al. 2005) onto the gold sensor surface. Each condition was analyzed by serial injections of 50 nM of specific target in 5x saline-sodium citrate (5xSSC) hybridization buffer (Carrascosa et al. 2009; Carrascosa et al. 2012). After each hybridization event, isoform-probe interactions were disrupted by using a 50% formamide aqueous solution (Fuchs et al. 2010) in order to free the DNA-probe for replicate measurements with the same biosurface. As shown in Fig. S1A, 20:1 ratio remarkably improved the accessibility of the targets to their complementary DNA-probes, increasing capture efficiency in 70% and 50% for *Fas56* and *Fas57* capture probes respectively. However, they had a notably high cross-hybridization from the non-specific isoforms, showing percentages of cross-hybridization from the off-target transcripts of 169% (*Fas567* probe) and 47% (*Fas57* probe). The evident preference of *Fas567* probe for *Fas57* isoform over *Fas567* isoform at all of the ratios tested made indispensable the avoidance of such crosshybridization in order to achieve a specific recognition.

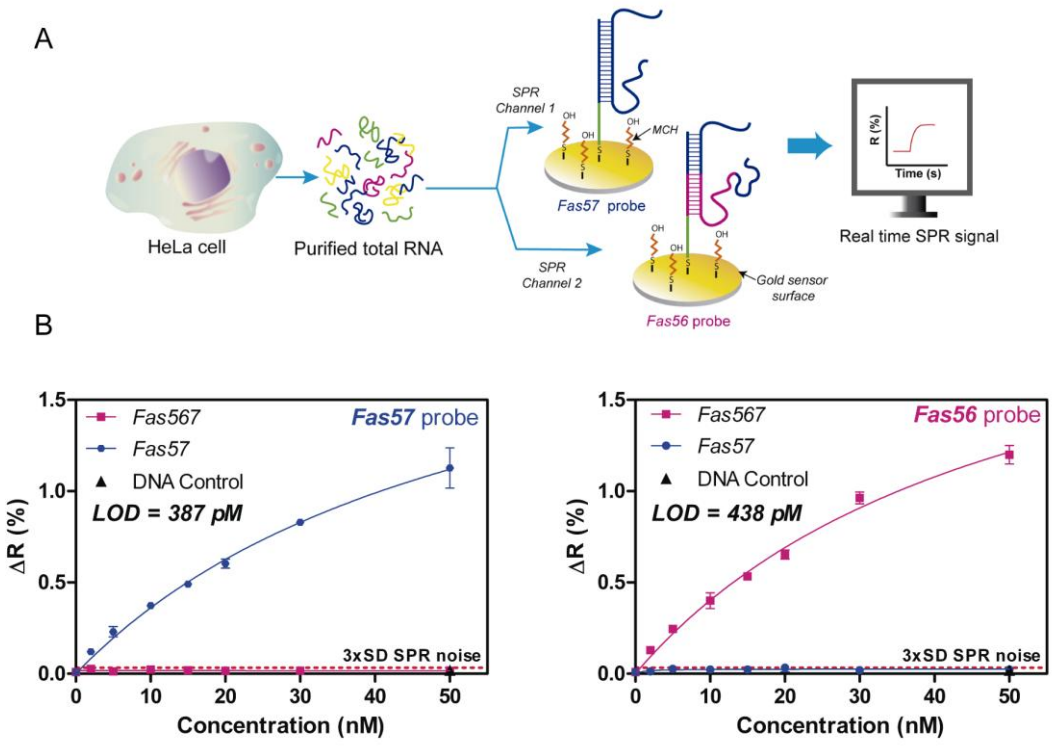

Fig. 2. SPR methodology for quantitative evaluation of *Fas* gene alternatively spliced mRNA isoforms. (A) Scheme for the label-free and direct detection of alternative spliced variants with an SPR biosensor. (B) SPR calibration plots for *Fas57* (*left*) (R^2= 0.99) and *Fas56* (*right*) (R^2=0.99) DNA-probes using the optimized hybridization and detection conditions. Solid lines (blue and pink) correspond to the non-linear fit of the calibration curves. Red dashed line corresponds to 3xSD SPR noise, which is the limit for the minimum signal detectable. All data show mean ± standard deviation (SD) of triplicate measurements.

Taking advantage of the capacity of formamide for destabilizing nucleic acid duplexes and increasing hybridization stringency (Fuchs et al. 2010) we studied its effect in the off-target/probe interaction at different concentrations (from 25% to 65%). The addition of formamide had a drastic effect on specificity, leveraging the sensitivity of the specific targets compared to the alternative ones in more than 75% (Fig. S1B). It was particularly evident with the *Fas56* probe, which presented an extensive cross-hybridization of the *Fas57* isoform in the absence of formamide. Furthermore, there was an increment in the target signal, corroborating the enhancing effect of formamide for the hybridization of oligonucleotides to their specific DNA-probes in saline solutions (Fuchs et al. 2010). To further improve the specific detection, we carried out a slight adjustment in the saline concentration of the hybridization buffer, reducing the cross-hybridization to background levels (Fig. S1C). Changes in the ionic strength of the hybridization buffer led to an increase in the stringency, decreasing the likelihood of hybridization and thus favoring binding of the fully complementary isoforms over non-fully complementary ones (Gong and Levicky 2008; Špringer et al. 2010).

After applying the optimized conditions, we were able to accurately discriminate between the different splicing isoforms while retaining high sensitivity. We achieved sensitivity levels at the pM-nM range as depicted in the calibration curves (Fig. 2B). Cross-hybridization was negligible even at the highest concentration evaluated of non-cognate transcripts (50 nM). We obtained LODs of 387 pM (R^2 = 0.99) for isoform

Fas57 and 438 pM (R^2 = 0.99) for *Fas567* and limits of quantification (LOQ), i.e. the lower limit of quantification, of 1.3 nM and 1.5 nM, respectively.

3.2. *Repeatability and reproducibility*

To demonstrate the robustness of the biosensor methodology, we assessed its repeatability and reproducibility, key parameters in the development of a reliable tool for analytical purposes. We determined the Coefficient of Variability (CV) of the signal for different target concentrations both within the same sensor chip (intra-assay) and among different biofunctionalization processes (inter-assay). In addition, we studied the variability between two different operators. Table 1 shows the CVs calculated for four concentrations (2, 5, 10 and 30 nM) of the isoforms located in the linear range of the calibration curves. The intra-assays showed a signal variation well-below the maximum variability recommended for analytical methods (~15%) (Wood 1999), with CVs between 2-11 %. Target detection maintained a stable response through at least 80 regeneration cycles with no notable signal loss compared to initial values (3 %CV) (**Fig. S2**). Furthermore, the reproducibility was markedly accurate even when measurements were carried out by different operators, obtaining CVs between 5-9 % and LODs with a variability of 1-11% in the inter-assay analysis. This statistical analysis proves the robustness of the methodology and its potential use in environments such as clinical settings, where simple, highly accurate and reproducible approaches are the main requirements. In addition, the consistency of these results is a unique advantage of this methodology, making it possible to analyze a set of samples with the same sensor-chip,

thereby saving time and resources and minimizing the experimental errors that could arise from different assays.

Table 1. Variability of the SPR sensor signals for *Fas* isoforms intra- and inter-assays performed by different operators. All p-values indicated not significant variation between the measurements (*P>0.05*, one-way ANOVA test).

Concentration (nM)	**ΔR(%)**							
	Intra-assay 1 [a]		***Intra-assay 2*** [a]		***Intra-assay 3*** [b]		***Inter-assay*** [ab]	
***Fas567* isoform**	**Mean±SD**[1]	**CV(%)**	**Mean±SD**[1]	**CV(%)**	**Mean±SD**[1]	**CV(%)**	**Mean±SD**[2]	**CV(%)**
2	0.13±0.01	8	0.13±0.01	9	0.14±0.01	4	0.13±0.01	9
5	0.24±0.01	4	0.20±0.01	6	0.25±0.01	2	0.23±0.02	9
10	0.38±0.02	4	0.35±0.01	3	0.39±0.02	6	0.38±0.02	6
30	0.96±0.03	3	0.98±0.05	5	0.99±0.08	8	0.98±0.05	5
LOD (pM)	438	-	516	-	423	-	459±50	11
***Fas57* isoform**	**Mean±SD**[1]	**CV(%)**	**Mean±SD**[1]	**CV(%)**	**Mean±SD**[1]	**CV(%)**	**Mean±SD**[2]	**CV(%)**
2	0.12±0.01	8	0.12±0.02	13	0.15±0.01	8	0.13±0.02	14
5	0.23±0.02	9	0.19±0.01	5	0.24±0.01	5	0.22±0.03	12
10	0.37±0.01	2	0.33±0.02	5	0.39±0.03	6	0.36±0.03	9
30	0.83±0.02	2	0.86±0.05	6	0.85±0.04	4	0.85±0.04	4
LOD (pM)	387	-	373	-	380	-	380±7	2

[a]Measurements performed by operator 1.
[b]Measurements performed by operator 2.
[1]Mean ± SD of 3 replicates performed in the same biofunctionalized sensor chip.
[2]Mean ± SD of 9 replicates performed in 3 different biofunctionalized sensor chips.

3.3. BCL-X alternative splicing detection

The development of a robust methodology that ensures the fidelity of specific splicing isoform detection with a minimized preset optimization is challenging. Thereby, we tested the versatility of our methodology in the detection of alternatively spliced isoforms from

the *BCL-X* gene. Deregulation of *BCL-X* gene (Lee et al. 2012) alternative splicing is involved in cancer development and can have an important impact in therapeutic decisions (Akgul et al. 2004). This gene has a three-exon structure and two 5'-alternative splice sites in the first coding exon, generating the *BCL-X_L* and *BCL-X_S* mRNA isoforms (Lee et al. 2012). When the upstream 5'-splice site is used, it generates the *BCLX_S* mRNA isoform, leading to a pro-apoptotic transmembrane protein. The use of the downstream 5' splice site leads to production of the anti-apoptotic *BCLX_L* mRNA isoform that encodes a large transmembrane protein (BCL-X_L) expressed in the mitochondrial membrane.

To analyze the mRNA expression levels of *BCL-X_L* and *BCL-X_S* isoforms, we followed the same SPR methodological approach using specific DNA-probes matching the splice-junctions (**Table S1**) and employed the optimized conditions developed for *Fas* gene detection described above. We obtained similar results to *Fas* gene (Fig. 3), achieving the same degree of specificity with near background levels of cross-hybridization. The LODs were 356 pM (R^2 = 0.99) for *BCLX_L* and 155 pM (R^2 = 0.99) for *BCL-X_S*, with LOQs of 1.2 nM and 0.5 nM respectively. Variability of the signals was below 15% for all concentration measured (**Table S2**), supporting the robustness of the methodology as an analytical tool for monitoring splicing events. Hence, the methodology was easily reproduced with the same efficiency, highlighting its potential as a tool for the monitoring of alternative splicing events of different genes and within different biological and eventually pathological contexts.

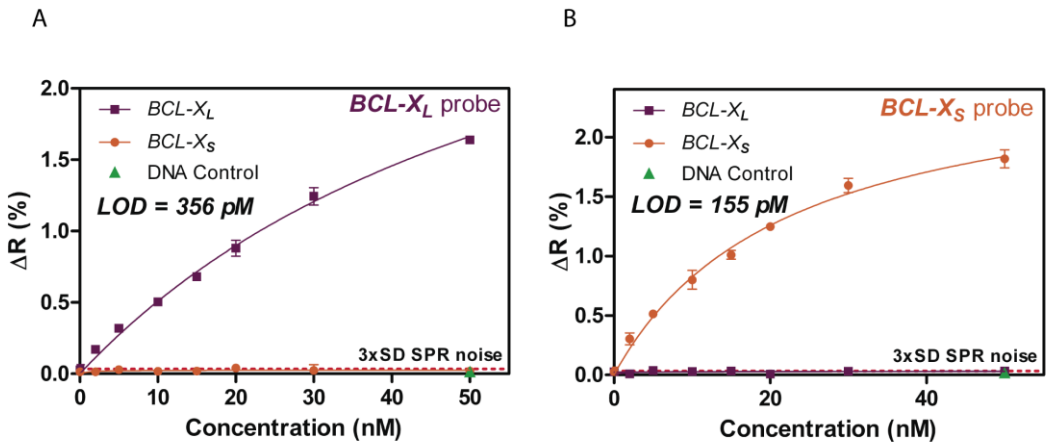

Fig. 3. SPR calibration plots for the detection of *BCL-X*$_L$ (*left*) (R^2= 0.99) and *BCL-X*$_S$ (*right*) (R^2= 0.99) synthetic isoforms based on the previously optimized detection conditions of *Fas* gene isoforms. Solid lines (blue and pink) correspond to the non-linear fit of the calibration curves. Red dashed line corresponds to 3xSD SPR noise, which is the limit for the minimum signal detectable. All data show mean ± SD of triplicate measurements.

3.4. *Experimental validation of Fas alternative splicing with HeLa cells*

To study the feasibility of the methodology in biological samples, we first tested it in ideal conditions. We purified total RNA from HeLa cells transfected with a minigene expressing *Fas* genomic sequences between exons 5 and 7 (~2000 nucleotide primary trancripts), either alone or co-transfected with a vector expressing the Polypyrimidine-Tract-Binding protein (PTB). Previous studies show that PTB induces skipping of *Fas* exon 6 acting through an exonic silencer sequence (Izquierdo et al. 2005). While expression of the minigene alone leads to preferential accumulation of exon 6-including transcripts, co-expression of *Fas* 567 minigene with PTB leads to higher accumulation of transcripts that skip exon 6 (Förch et al. 2000). In this study, mature transcripts from the transfected minigene generated *Fas* isoforms with approximately similar lengths to those employed during the optimization. Thus, we quantified the minigene expression in

both cell lines by applying the conditions and calibration curves generated during the optimization process.

Samples were diluted in 3xSSC (45% FA) to a final concentration of 20 ng/µL of purified total RNA. We used purified total RNA from bacteria (XLI Blue) as a negative control and we also evaluated the response of HeLa cells expressing only endogenous levels of *Fas* transcripts. Shifts in isoform ratios were independently evaluated for each HeLa cell line by RT-PCR using primers corresponding to the flanking constitutive exons and quantification of the amplification products corresponding to the alternative transcript after fractionation by polyacrylamide gel electrophoresis or by RT-qPCR using isoform-specific primers.

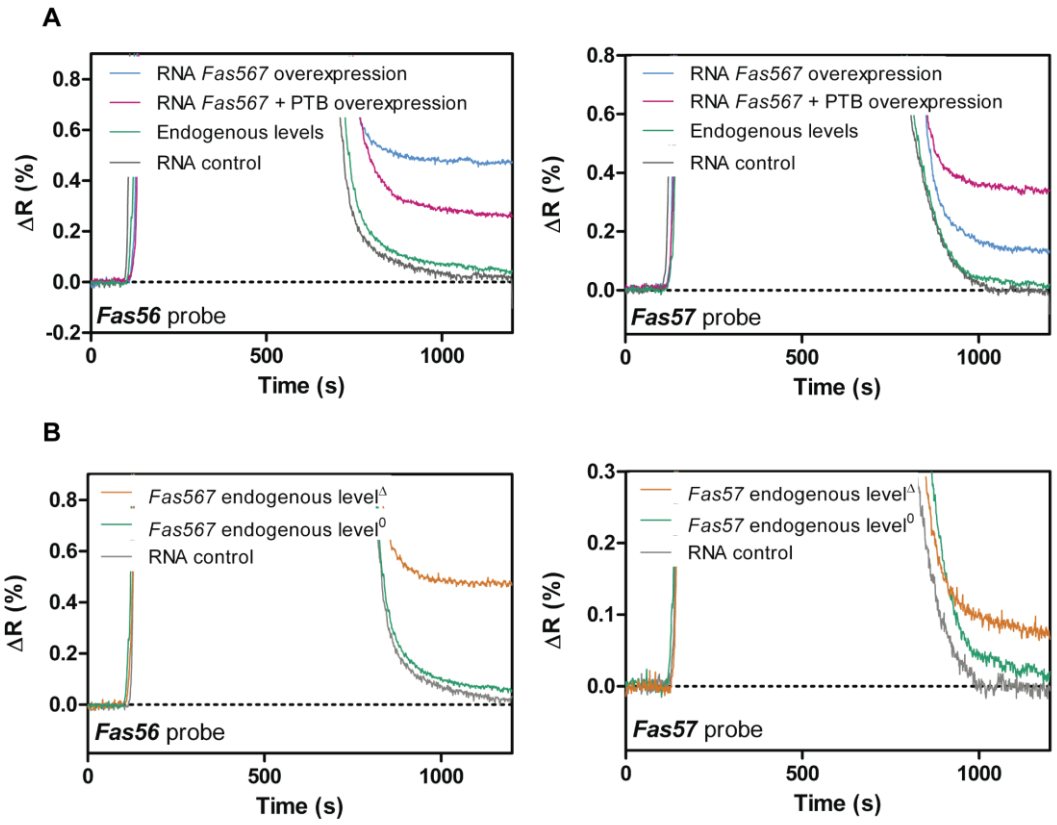

Fig. 4. SPR sensograms of the detection of 20 ng/ µL of total HeLa cell RNA for: (A) Minigene-expression for both DNA-probes, *Fas56* (*left*) and *Fas57* (*right*) and (B) Endogenous expression of these isoforms either with RNA hydrolysis (Δ) and without any treatment (0), detected for both DNA-probes, *Fas56* (*left*) and *Fas57* (*right*).

As can be observed in both sensograms (Fig. 4A), mRNAs generated by the expression of the transfected minigenes were clearly detected by the SPR biosensor. Bacteria RNA control samples showed zero ΔR (%) while samples from minigene-tranfected HeLa-cells presented a ΔR (%) higher than zero for both isoforms, indicating specific detection of the *Fas* isoforms. Isoforms from HeLa cells expressing only endogenous levels of *Fas* transcripts were not detected under these conditions. Expression of the 567 minigene led to higher detection levels of *Fas567* isoform compared to *Fas57* isoform, while co-expression of the 567 minigene and PTB expression vector led to higher detection of the *Fas57* isoform compared to the *Fas567* isoform, as previously reported (Izquierdo et al. 2005) and independently validated in these experiments (**Fig. S3A**). SPR responses were converted to quantitative data by their direct interpolation in the calibration curves. These values were also corrected with their respective dilution factors with respect to the particular total RNA concentration of each sample. SPR quantitative data correlated very closely with the quantitative data obtained with RT-qPCR for the minigene products (Table 2). Both, RT-qPCR and SPR techniques, showed an exon-skipping shift of 37% and 38% respectively after co-expression with PTB. 567/57 ratios were fairly comparable between both techniques with values of 2.2 (RT-qPCR) and 2.5 (SPR) for *Fas567* overexpression and 0.38 (RT-qPCR) and 0.45 (SPR) with PTB co-expression. Both techniques showed a high correlation (r = 0.97) and all data was found within the limits of agreement (**Fig. S5A**). We conclude that the SPR biosensor data were fully validated by independent quantitative measurements under these ideal conditions.

Table 2. RT-PCR and SPR comparison of the isoform content analysis from HeLa cells endogenous expression and minigene-induced overexpression. Isoform concentration in nM for SPR was calculated through the calibration curves obtained for each DNA-probe according to their ΔRs (%).

Sample type	*Fas* isoform	Concentration (nM)		567/ 57ratio	
		RT-qPCR	SPR	RT-qPCR	SPR
RNA *Fas567* overexpression	**567**	205	240 ± 23[a]	2.2	2.5 ± 0.3
	57	93	97 ± 23[a]		
RNA *Fas567* overexp. + PTB	**567**	75	92 ± 14[a]	0.38	0.45 ± 0.06
	57	199	204 ± 22[a]		
***Fas* endogenous levels**	**567**	365	262 ± 27[Δ]	17.9	22.9 ± 1.4
	57	20	12.0 ± 0.8[Δ]		

[Δ]Mean ± SD of the concentration obtained in SPR from 2 different measurements from purified samples of HeLa cell's total RNA after alkaline hydrolysis.
[a]Mean ± SD of three independent SPR measurements.

The deficient detection of endogenous HeLa cell *Fas* RNAs was possibly due to the much longer length of the *Fas* transcripts endogenous isoforms. Target sizes is an important factor in optical biosensors based on refractive index changes on solid surfaces because of the generation of complex secondary structures that can hinder their accessibility to the monolayer, as reviewed elsewhere (Šípová and Homola 2013). To circumvent this potential problem, we introduced a step of RNA fragmentation before the detection of endogenous isoforms by partial hydrolysis of the RNA. Because alkaline hydrolysis has been used for different purposes such as the detection of cell-extracted 16S rRNAs using SPR imaging (Nelson et al. 2002) or as a tool for genome-wide mapping of RNA (Wan et al. 2013), we attempted RNA fragmentation using this method. The time of hydrolysis was optimized as previously described (Wan et al. 2013) to obtain RNA fragments of the desired length (~200nt), evaluated by agarose gel electrophoresis (**Fig. S4**) at 3.5 min of RNA treatment. To monitor the isoform levels,

duplicate measurements were carried out in the SPR sensor. Samples were diluted in 3xSSC (45% FA) to 20 ng/µL of purified total RNA. Isoform concentrations were calculated by interpolation of the sensor signal to the calibration curves obtained for each DNA-probe. In parallel, RT-PCR assays and agarose gel electrophoresis (**Fig. S3B**) and RT-qPCR (Table 2) were carried out using the same samples for validation of the biosensor data. Fig. 4B shows the SPR sensograms obtained after injection of HeLa RNA samples for each DNA-probe. As can be seen, endogenous RNAs generated readily detectable signals above background, confirming our hypothesis that RNA fragmentation can increase the detection signals by SPR. The results of Table 2 show that SPR data generated a slight underestimation of isoform concentrations with respect to RT-qPCR quantification. This different quantification may be due to incomplete (or excessive) cleavage by the fragmentation protocol applied, suggesting that a further optimization of the hydrolysis could generate better matches between SPR and RT-qPCR values. Due to this underestimation, the correlation between both techniques was lower in comparison to ideal conditions (r = 0.86) (**Fig. S5B**). However, 83% of the samples tested (5/6) were found within the limits of agreement. Importantly, a comparison of the ratios between isoforms revealed comparable values for the two techniques, 17.9 for RT-qPCR and 22.9 for SPR. Indeed, isoform ratios showed a very significant correlation (r = 0.99) and presented a 100% validation ratio (3/3) between both techniques (**Fig. S5C**). Far from compromising RNA detection by SPR, RNA hydrolysis helped to establish a more general methodology for studying alternative splicing processes through SPR biosensor by unifying isoform lengths. Although incomplete fragmentation led to a slight underestimation of the actual concentration of both isoforms compared to RT-qPCR results, a more accurate setting of the fragmentation protocol may further improve the quantification. Estimation of the ratio

between alternative spliced isoforms is generally a key for assessing splicing deregulation, highlighting the methodology as an appropriate tool for disease diagnosis or prognosis. Furthermore, this methodology can be easily implemented to more advanced label-free optical biosensor platforms which have demonstrated higher sensitivity and multiplexing capabilities than SPR biosensors such those based on photonic interferometers (Duval et al. 2012), offering a much more detailed information and opening the possibility for the development of new tools for diagnosis and follow-up therapies.

4. Conclusions

We present a methodology for monitoring mRNA isoforms produced by alternative splicing events in real-time employing a portable SPR biosensor. It involves minimal sample manipulation and avoids the use of labels or pre-amplification steps in contrast with the current gold standard RT-qPCR technique which is prone to introduce bias due to the cDNA conversion and amplification processes. Our methodology strictly discriminates against the non-complementary isoforms in the pM-nM range. It has been proven to be easily reproduced with the same efficiency when it is applied to a different gene, highlighting its feasibility as a tool for the monitoring of alternative splicing events of different genes and within different biological and pathological contexts. This advantage reduces greatly the time and material employed during experimental setups and, therefore, minimizes the cost. Moreover, it reduces the systematic errors arisen from different probe affinities in the amplification process, leading to a more reliable analysis.

The feasibility of the methodology was tested in complex RNA mixture purified from HeLa cells transfected and not transfected with various DNA expression constructs. Results strongly correlated with RT-qPCR data. Additionally, the biosensor can be reused up to 80 hybridization/regeneration cycles with no apparent signal loss, which demonstrates its robustness and reproducibility for long-term use.

The simplicity of our SPR methodology, along with the label free detection and the minimized sample manipulation, makes it really useful for the real-time monitoring of splicing events. In our view, these results open the door for this tool to be routinely employed for the analysis of alternatively spliced mRNA isoforms as biomarkers for diagnosis and patient follow-ups during therapy, providing a more informative, specific and accurate analysis.

Acknowledgments

Work in JV's lab was supported by Fundación Botín, by Banco de Santander through its Santander Universities Global Division and by Consolider RNAREG, MICINN and AGAUR.

Work in L.M.L.'s lab was financially supported by Fundación Botín and EPISENS project of the Spanish Ministry of Science and Innovation (TEC2012-3428). The nanoB2A is a consolidated research group (Grup de Recerca) of the Generalitat de Catalunya and has support from the Departament d'Universitats, Recerca i Societat de la Informació de la Generalitat de Catalunya (2014 SGR 624). ICN2 acknowledges support of the Spanish MINECO through the Severo Ochoa Centers of Excellence Program under Grant SEV-2013-0295.

References

Akgul, C., Moulding, D., Edwards, S., 2004. Cell Mol Life Sci. 61(17), 2189-2199.

Boroumand-Noughabi, S., Sima, H., Ghaffarzadehgan, K., Jafarzadeh, M., Raziee, H., Hosseinnezhad, H., Moaven, O., Rajabi-Mashhadi, M., Azarian, A., Mashhadinejad, M., Tavakkol-Afshari, J., 2010. BMC Cancer 10(275).

Boucard, D., Toulmé, J., Di Primo, C., 2006. Biochemistry 45(5), 1518-1524.

Braunschweig, U., Gueroussov, S., Plocik, A.M., Graveley, B.R., Blencowe, B.J., 2013. Cell 152(6), 1252-1269.

Carrascosa, L.G., Calle, A., Lechuga, L.M., 2009. Anal Bioanal Chem 393, 1173-1182.

Carrascosa, L.G., Gómez-Montes, S., Aviñó, A., Nadal, A., Pla, M., Eritja, R., Lechuga, L., 2012. Nucleic Acids Res 40(8), e56.

Cascino, I., Fiucci, G., Papoff, G., Ruberti, G., 1995. J. Immunol. 154, 2706-2713.

Cheng, J., Zhou, T., Liu, C., Shapiro, J.P., Brauer, M.J., Kiefer, M.C., Barr, P.J., Mountz, J.D., 1994. Science 263, 1759-1762.

David, C., Manley, J., 2010. Genes Dev. 24(21), 2343-2364.

Duval, D., González-Guerrero, A.B., Dante, S., Osmond, J., Monge, R., Fernández, L.J., Zinoviev, K.E., Domínguez, C., Lechuga, L.M., 2012. Lab on a Chip 12(11), 1987-1994.

Förch, P., Puig, O., Kedersha, N., Martínez, C., Granneman, S., Séraphin, B., Anderson, P., Valcárcel, J., 2000. Molecular Cell 6(5), 1089-1098.

Fuchs, J., Dell'Atti, D., Buhot, A., Calemczuk, R., Mascini, M., Livache, T., 2010. Analytical biochemistry 397(1), 132-134.

Ghigna, C., Valacca, C., Biamonti, G., 2008. Curr Genomics 9, 556-570.

Gong, P., Levicky, R., 2008. Proceedings of the National Academy of Sciences 105(14), 5301-5306.

Izquierdo, J., Majós, N., Bonnal, S., et al., 2005. Mol. Cell 19(4), 475-484.

Joung, H., Lee, N., Lee, S., Ahn, J., Shin, Y., Cho, i.H., Lee, C., Kim, S., Kim, M., 2008. Anal Chim Acta. 630(2), 168-173.

Krammer, P.H., 2000. Nature 407(6805), 789-795.

Lee, H., Wark, A., Corn, R., 2008. Analyst. 133(5), 596-601.

Lee, J., Zhou, J., Zheng, X., Cho, S., Moon, H., Loh, T., Jo, K., Shen, H., 2012. Biochem Biophys Res Commun 420(2), 467-472.

Lee, K., Cui, Y., Lee, L.P., Irudayaraj, J., 2014. Nature nanotechnology 9(6), 474-480.

Lee, Y., Rio, D.C., 2015. Annual review of biochemistry 84(1).

Li, Y.-J., Xiang, J., Zhou, F., 2007. Plasmonics 2(2), 79-87.

Mandir, J.B., Lockett, M.R., Phillips, M.F., Allawi, H.T., Lyamichev, V.I., Smith, L.M., 2009. Anal Chem. 81(21), 8949-8956.

Nair, T.M., Myszka, D.G., Davis, D.R., 2000. Nucleic Acids Res. 28(9), 1935-1940.

Nasheri, N., Cheng, J., Singaravelu, R., Wu, P., McDermott, M., Pezacki, J., 2011. Anal Biochem. 412(2), 165-172.

Nelson, B., Liles, M., Frederick, K., Corn, R., Goodman, R., 2002. Environ Microbiol. 4(11), 735-743.

Nilsen, T.W., Graveley, B.R., 2010. Nature 463(7280), 457-463.

Oltean, S., Bates, D., 2014. Oncogene 33(46), 5311-5318.

Owen-Schaub, L., Chan, H., Cusack, J.C., Roth, J., Hill, L.L., 2000. Int. J. Oncol. 17(1), 5-12.

Owen-Schaub, L.B., van Golen, K.L., Hill, L.L., Price, J.E., 1998. J. Exp. Med. 188(9), 1717-1723.

Padgett, R.A., 2012. Trends in Genetics 28(4), 147-154.

Pan, Q., Shai, O., Lee, L.J., Frey, B.J., Blencowe, B.J., 2008. Nature Genet. 40, 1413-1415.
Sakao, Y., Nakamura, F., Ueno, N., Hara, M., 2005. Colloids and Surfaces B: Biointerfaces 40(3–4), 149-152.
Šípová, H., Homola, J., 2013. Analytica Chimica Acta 773(0), 9-23.
Sipova, H., Zhang, S., Dudley, A.M., Galas, D., Wang, K., Homola, J., 2010. Analytical Chemistry Article ASAP.
Spitali, P., Aartsma-Rus, A., 2012. Cell 148(6), 1085-1088.
Špringer, T., Šípová, H., Vaisocherová, H., Štěpánek, J., Homola, J., 2010. Nucleic Acids Research.
Tazi, J., Bakkour, N., Stamm, S., 2009. Biochimica et Biophysica Acta (BBA) - Molecular Basis of Disease 1792(1), 14-26.
Vaisocherová, H., Zítová, A., Lachmanová, M., Tpánek, J., Králíková, á., Liboska, R., Rejman, D., Rosenberg, I., Homola, J., 2005. Biomolecules at Surfaces 82(4), 394 - 398.
Wan, Y., Qu, K., Ouyang, Z., Chang, H.Y., 2013. Nature protocols 8(5), 849-869.
Wang, E.T., et al., 2008. Nature 456, 470-476.
Wood, R., 1999. TrAC Trends in Analytical Chemistry 18(9–10), 624-632.
Wu, Y.-M., Kung, S.-S., Chow, W.-Y., 1996. FEBS Letters 390, 157-160.
Xing, Y., Stoilov, P., Kapur, K., Han, A., Jiang, H., Shen, S., Black, D.L., Wong, W.H., 2008. Rna 14(8), 1470-1479.
Zhang, Z., Pal, S., Bi, Y., Tchou, J., Davuluri, R., 2013. Genome Med 5(4), 33.
Zhou, W., Chen, Y., Corn, R., 2011. Anal Chem 83(10), 3897-3902.

Table 1. Variability of the SPR sensor signals for *Fas* isoforms intra- and inter-assays performed by different operators. All p-values indicated not significant variation between the measurements (*P>0.05*, one-way ANOVA test).

Concentration (nM)	**ΔR(%)**							
	Intra-assay 1 [a]		***Intra-assay 2*** [a]		***Intra-assay 3*** [b]		***Inter-assay*** [ab]	
***Fas567* isoform**	**Mean±SD[1]**	**CV(%)**	**Mean±SD[1]**	**CV(%)**	**Mean±SD[1]**	**CV(%)**	**Mean±SD[2]**	**CV(%)**
2	0.13±0.01	8	0.13±0.01	9	0.14±0.01	4	0.13±0.01	9
5	0.24±0.01	4	0.20±0.01	6	0.25±0.01	2	0.23±0.02	9
10	0.38±0.02	4	0.35±0.01	3	0.39±0.02	6	0.38±0.02	6
30	0.96±0.03	3	0.98±0.05	5	0.99±0.08	8	0.98±0.05	5
LOD (pM)	438	-	516	-	423	-	459±50	11
***Fas57* isoform**	**Mean±SD[1]**	**CV(%)**	**Mean±SD[1]**	**CV(%)**	**Mean±SD[1]**	**CV(%)**	**Mean±SD[2]**	**CV(%)**
2	0.12±0.01	8	0.12±0.02	13	0.15±0.01	8	0.13±0.02	14
5	0.23±0.02	9	0.19±0.01	5	0.24±0.01	5	0.22±0.03	12
10	0.37±0.01	2	0.33±0.02	5	0.39±0.03	6	0.36±0.03	9
30	0.83±0.02	2	0.86±0.05	6	0.85±0.04	4	0.85±0.04	4
LOD (pM)	387	-	373	-	380	-	380±7	2

[a]Measurements performed by operator 1.

[b]Measurements performed by operator 2.

[1]Mean ± SD of 3 replicates performed in the same biofunctionalized sensor chip.

[2]Mean ± SD of 9 replicates performed in 3 different biofunctionalized sensor chips.

Table 2. RT-PCR and SPR comparison of the isoform content analysis from HeLa cells endogenous expression and minigene-induced overexpression. Isoform concentration in nM for SPR was calculated through the calibration curves obtained for each DNA-probe according to their ΔRs (%).

Sample type	*Fas* isoform	Concentration (nM)		567/ 57ratio	
		RT-qPCR	SPR	RT-qPCR	SPR
RNA *Fas567* overexpression	567	204.6	240 ± 23[a]	2.2	2.5 ± 0.3
	57	93.2	97 ± 23[a]		
RNA *Fas567* overexp. + PTB	567	74.9	92 ± 14[a]	0.38	0.45 ± 0.06
	57	198.8	204 ± 22[a]		
Fas endogenous levels	567	365	262 ± 27[Δ]	17.9	22.9 ± 1.4
	57	20.3	12.0 ± 0.8[Δ]		

[Δ]Mean ± SD of the concentration obtained in SPR from 2 different measurements from purified samples of HeLa cell's total RNA after alkaline hydrolysis.

[a]Mean ± SD of three independent SPR measurements.

Fig 1

Click here to download high resolution image

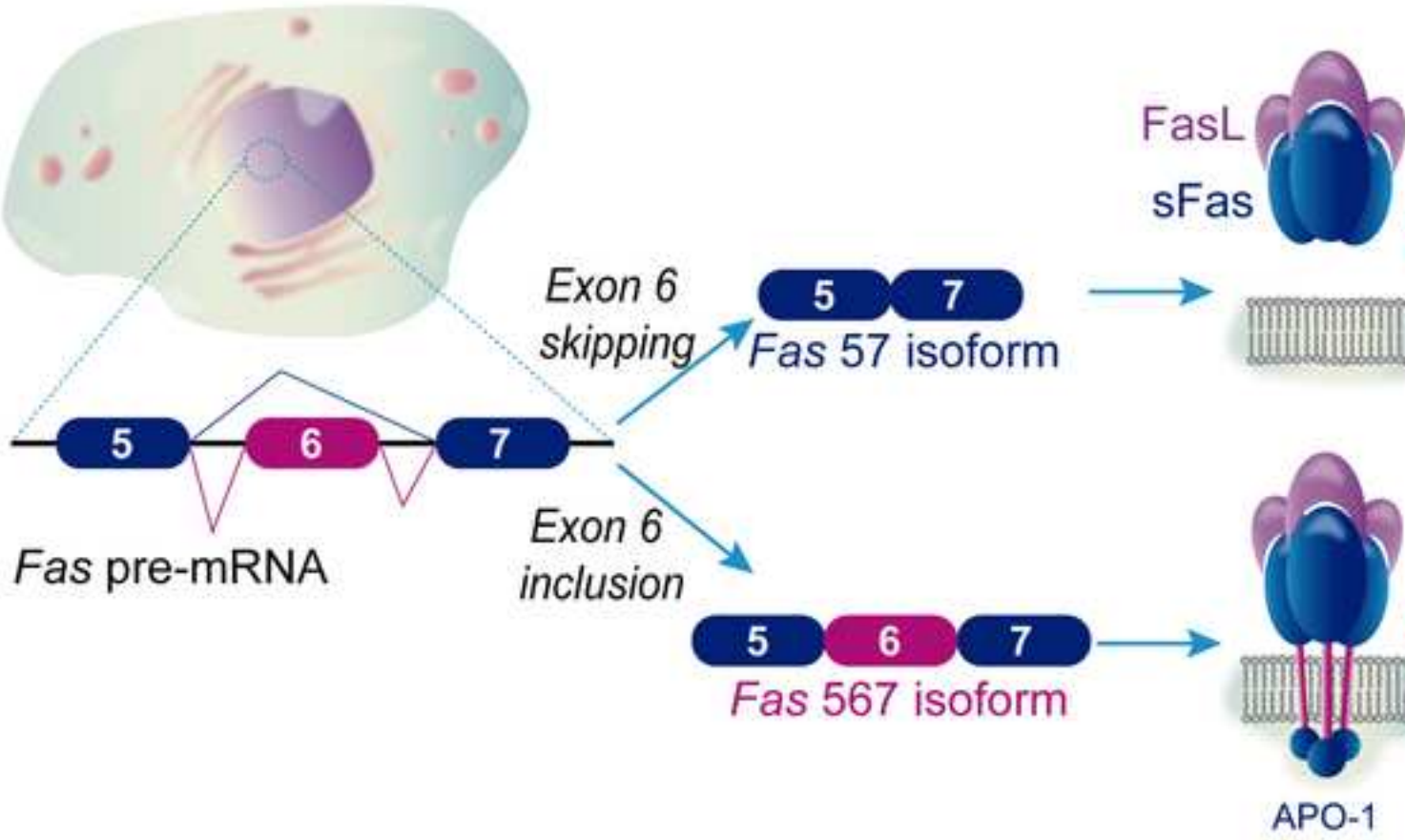

Fig 2

Click here to download high resolution image

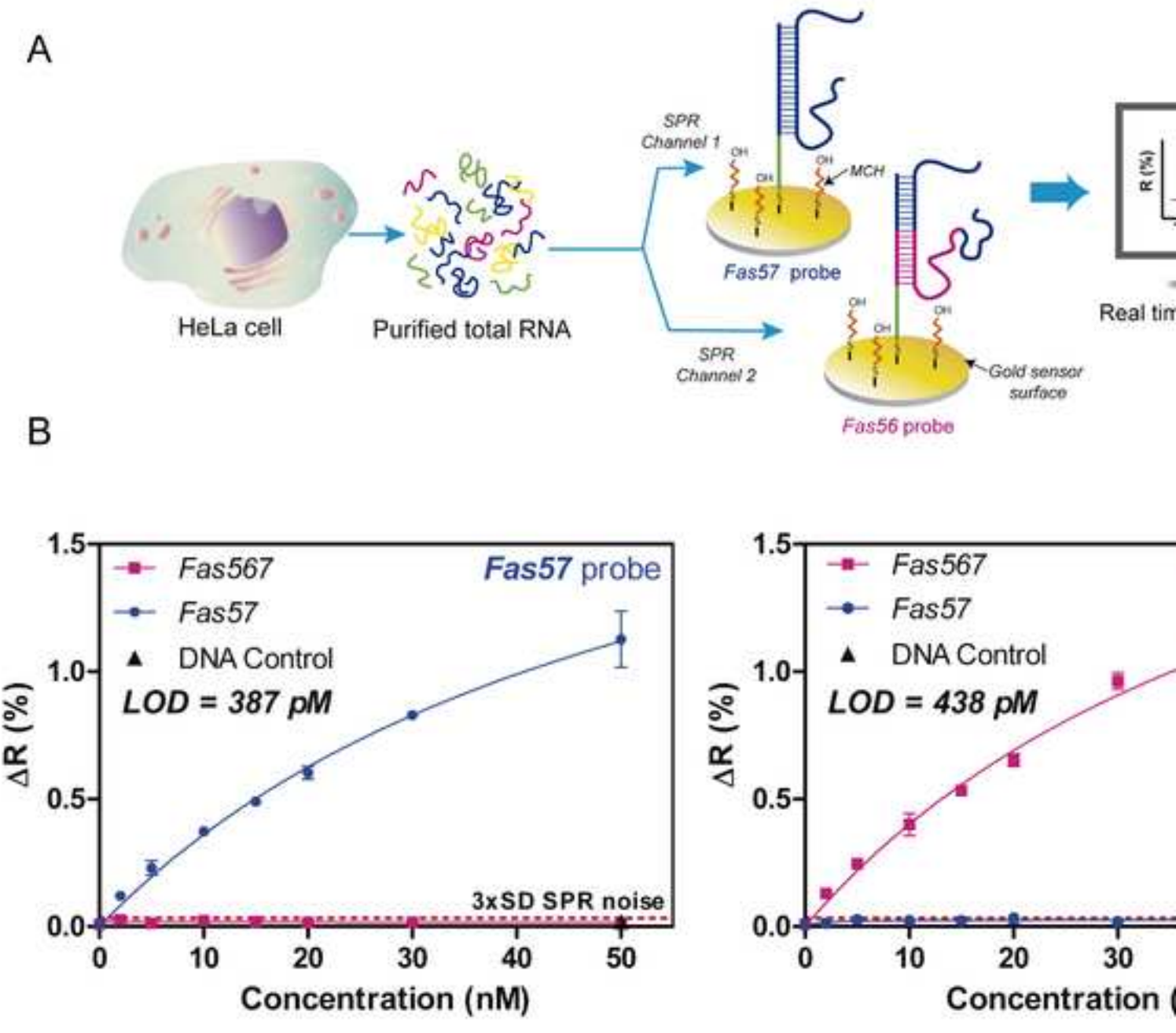

Fig 3

Click here to download high resolution image

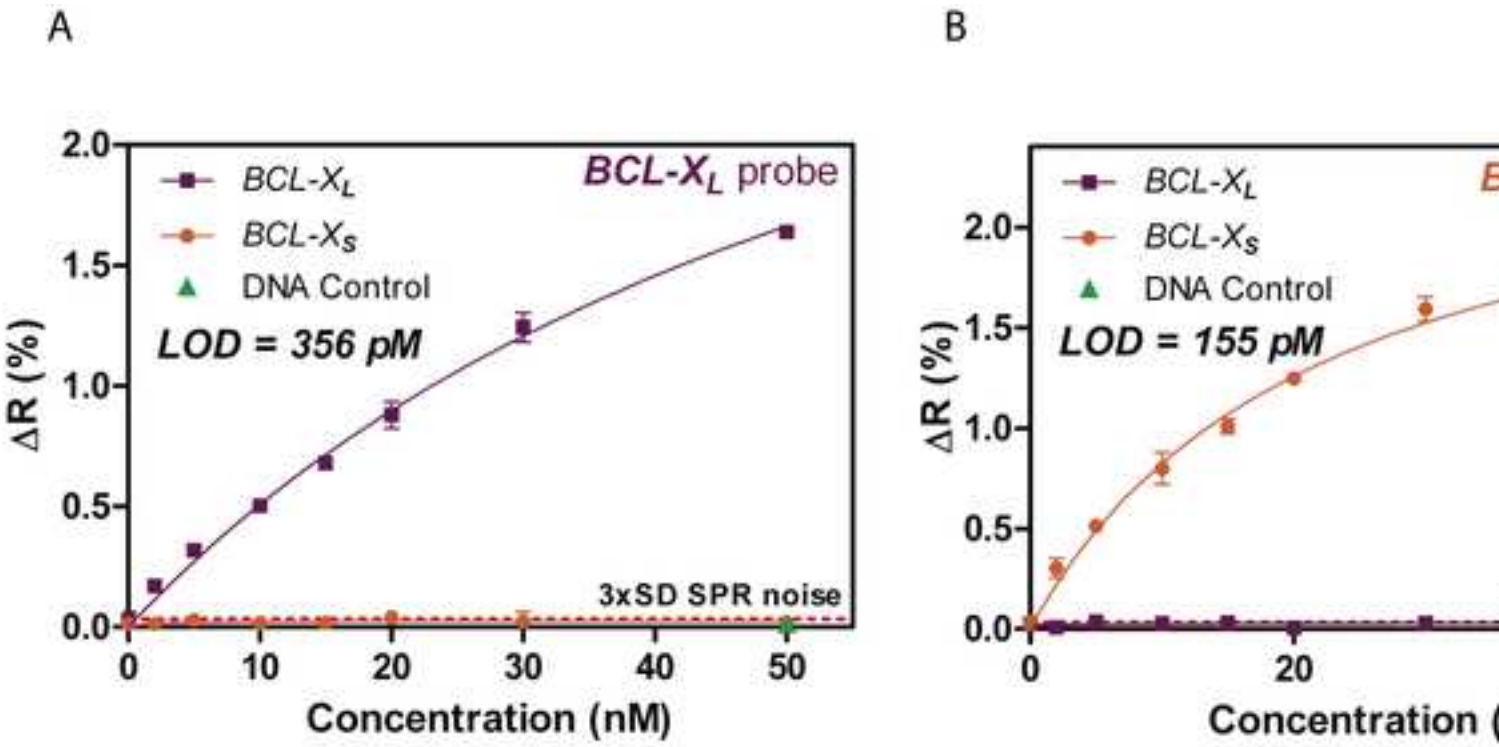

Figure 4

Click here to download high resolution image

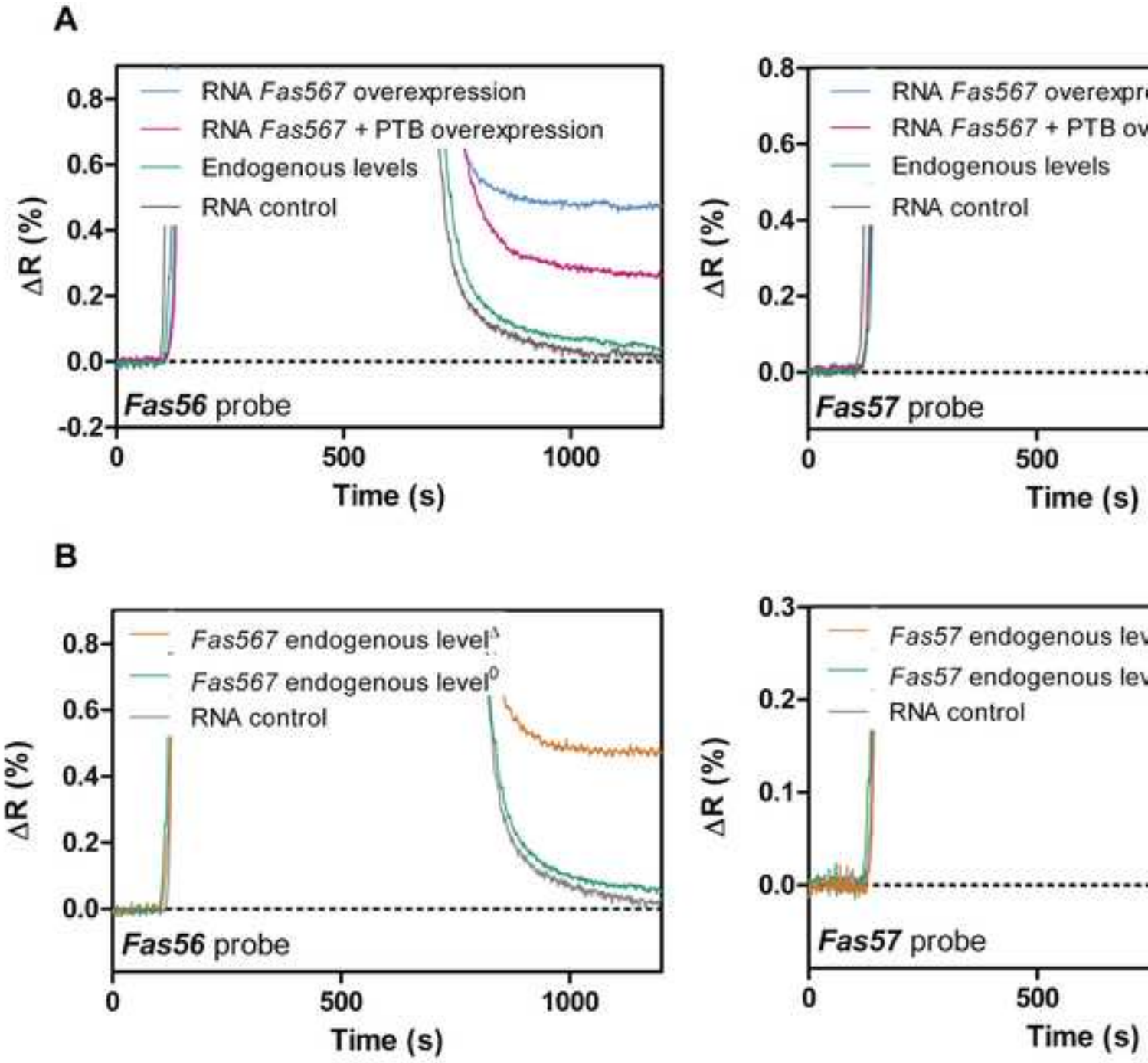

Supplementary Material

Click here to download Supplementary Material: Supplementary material SPR alternative splicing B&B.docx

***Highlights (for review)**

- A direct and label-free biosensing platform for alternative splicing monitoring is reported.

- Total discrimination against non-complementary isoforms was achieved reducing cross-hybridization to background levels.

- An RNA alkaline hydrolysis stepis performed to improve target accessibility and to establish a general methodology.

- Versatility of the methodology is demonstrated, being easily reproduced with the same efficiency when it is applied to a different gene.

- Results strongly correlated with RT-qPCR data, representing a useful tool for the real-time monitoring of splicing events